

Experimental evidence of the dominant role of low-angle grain boundaries for the critical current density in epitaxially grown $\text{YBa}_2\text{Cu}_3\text{O}_{7-\delta}$ thin films

S. Brück*

Max-Planck-Institut für Metallforschung, Heisenbergstrasse 3, D-70569 Stuttgart, Germany

J. Albrecht

*Max-Planck-Institut für Metallforschung, Heisenbergstrasse 3, D-70569 Stuttgart, Germany
and Max-Planck-Institut für Festkörperforschung, Heisenbergstrasse 1, D-70569 Stuttgart, Germany*

(Received 30 November 2004; published 24 May 2005)

Thin films of the high-temperature superconductor $\text{YBa}_2\text{Cu}_3\text{O}_{7-\delta}$ (YBCO) show an increase of the critical current density if grown on nanostructured SrTiO_3 (STO) substrate. The temperature dependence of the critical current density of such a film was measured and compared to $j_c(T)$ grown on regular [100] STO. The magneto-optical imaging technique was used to measure the flux-density distribution in the film and by applying an inversion scheme of the law of Biot and Savart the current density distribution in the film was calculated with a spatial resolution of $5 \mu\text{m}$. By comparing the results with theoretical models for the temperature dependence of j_c in conventional HTSC thin films, a possible explanation for the increase of the critical current density due to the nanostructuring is presented. In addition, a complete scenario is obtained of the pinning mechanisms in YBCO thin films epitaxially grown on STO for the investigated temperature range of $T=8-70$ K from the results.

DOI: 10.1103/PhysRevB.71.174508

PACS number(s): 74.25.Sv, 74.72.Bk, 74.78.Bz, 74.25.Qt

The effective pinning mechanisms of flux lines in epitaxially grown thin films of the high-temperature superconductor (HTSC) $\text{YBa}_2\text{Cu}_3\text{O}_{7-\delta}$ (YBCO) have been subject to much questioning. A promising approach to gain more information on the subject has been the investigation of the temperature dependence of the critical current density.¹⁻³ This has been done so far only on artificially disordered films with strongly reduced critical current density.^{4,5} Here a approach is presented by investigating the critical current density in YBCO thin films which show an increase of j_c in parts of the film due to nanostructuring of the surface of the substrate. It could be shown that a proper modification of the substrate surface can lead to a significant increase of the critical current density in the YBCO film.^{6,7} It will be shown that the investigation of the temperature dependence is a valuable method to identify the dominant mechanisms leading to the increased critical current density. Moreover a two-step power-law behavior for j_c can be observed which enables us to answer the question of the acting pinning mechanisms in epitaxially grown YBCO thin films in general.

The investigation of the temperature dependence of the critical current density is carried out on optimally doped thin films of the high-temperature superconductor YBCO. As substrate material, strontium titanate (STO) with a polished surface oriented along [100] direction is used. The irradiation with gallium ions under certain conditions allows creating well ordered structures on the substrate surface.^{8,9} For the samples presented here, a focussed ion beam (FIB) facility has been used for irradiation. The FIB provides gallium ions with an energy of 30 keV, a beam current of 1000 pA and a beam diameter of nominally 80 nm. It must be mentioned that for the actual irradiation process, the sample was coated with a 20 nm YBCO film to reduce surface charging effects, however this YBCO coating was removed by chemical etch-

ing directly after the irradiation. By irradiating a regular point grid with a point distance of 230 nm in both lateral directions and using a dwell time of 90 μs per irradiated dot a well ordered structure is created on the surface of the substrate. Figure 1 shows an atomic force microscopy image of the patterned substrate after removing the YBCO layer. The image has been taken using a *JPK Instruments NanoWizard AFM* in contact mode and shows an area of $2 \times 2 \mu\text{m}^2$ with an overall height of 11 nm. A linelike pattern with an approximate distance of 200 nm and a height of 3 nm is found. Since it is favorable to directly compare between YBCO grown on structured and on unstructured STO, only a part of the substrate has been treated in the above described manner, so the structured part on the surface has a size of $234 \times 202 \mu\text{m}^2$. After nanostructuring the substrate, the actual film was grown by pulsed laser deposition.¹⁰ The film has a thickness of $d=150$ nm and is optimally doped having a critical temperature of $T_c=90 \pm 1$ K. As final preparation step, a chemical etching process is performed to create square shaped films with lateral dimensions of $1 \times 1 \text{mm}^2$. Care has been taken so that the structured area lies well inside the resulting square shaped film.

The critical current density is measured by means of the magneto-optical Faraday effect.¹¹ The experimental setup consists of a ferrimagnetic lutetium-doped iron garnet film, which is placed on the superconducting film as the field sensing element. Such iron garnet films allow measuring the magnetic-flux density distribution with a resolution of better than $10 \mu\text{T}$ while providing a spatial resolution of better than $1 \mu\text{m}$.¹² The magnetic-flux density distribution of the whole superconductor may be imaged in one measurement using a charge-coupled device camera and a polarization microscope. From the resulting gray-scale images of the magnetic-flux density distribution in the superconductor, the current

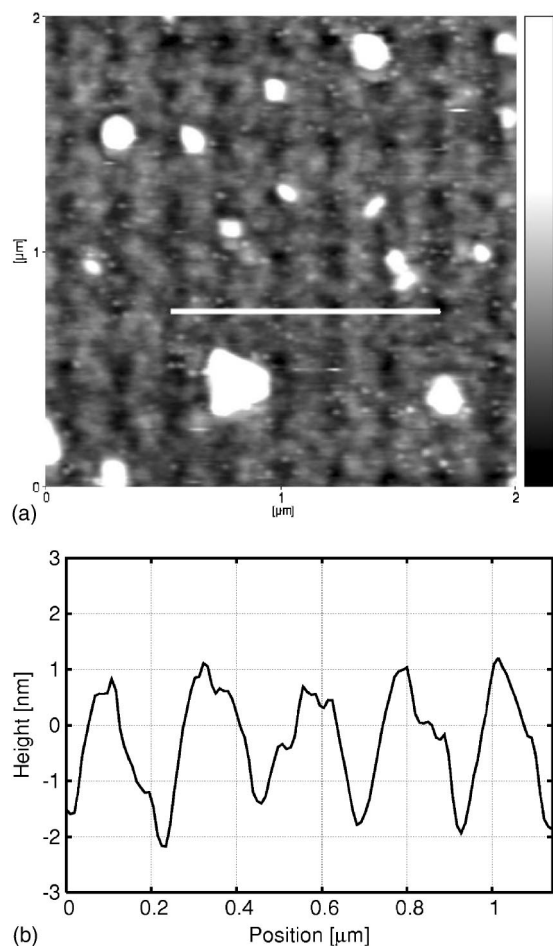


FIG. 1. Atomic force microscopy image of the surface of the STO substrate after structuring with the FIB using the values given in the text and removing the coating YBCO layer by chemical etching. The image shows an area of $2 \times 2 \mu\text{m}^2$ and has a total height of 11 nm. The graph below shows the profile indicated in the image by a white line. The white dots refer to remnants of the YBCO layer.

density distribution can be calculated by an inversion scheme of the law of Biot and Savart.¹³ Assuming a two-dimensional current-density distribution $\vec{j}(j_x, j_y, 0)$ in the film, the law of Biot and Savart can be inverted unambiguously. To consider the influence of an in-plane component of the external magnetic field caused by the supercurrent itself, an iteration method, according to Laviano *et al.*, has been applied to the calculations.¹⁴ Finally, the current density distribution in the YBCO film can be obtained with high accuracy and a spatial resolution of about $6 \mu\text{m}$.

The samples are zero-field cooled to $T=7$ K, then an external field of $B_{\text{ext}}=240$ mT is applied for $t=5$ s to create vortices throughout the whole sample. The actual measurement is carried out by acquiring images of the flux-density distribution in steps of 1 K in the range from $T=8-70$ K. The sample is in the vortex state and there is no external field applied during the measurement. To avoid problems resulting from relaxation processes of the vortices, for each temperature a constant delay time is chosen before acquiring the image.¹⁵ The obtained flux density distributions are then converted into current densities by the above-mentioned numeri-

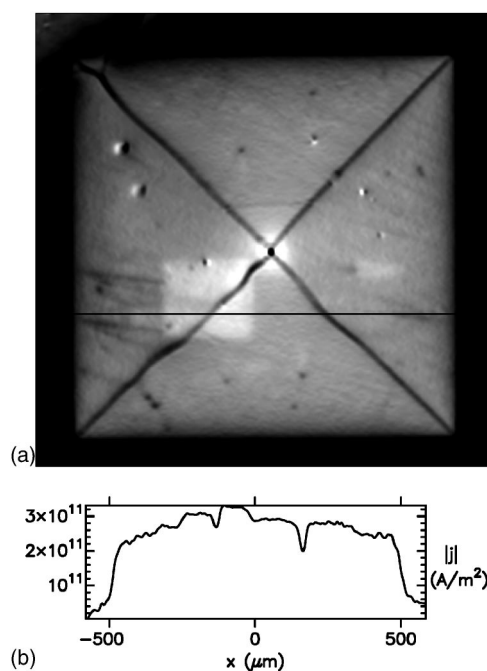


FIG. 2. Gray-scale image of the critical current density distribution in the square-shaped YBCO film. The superconductor is in the critical state with no external field being applied at a temperature of $T=8$ K. The superconductor shows an enhanced current density on the structured part of the substrate. The black line indicates the position of the current density profile given in the graph below the image.

cal inversion scheme. Figure 2 shows the resulting gray-scale image of the critical current density distribution at a temperature of $T=8$ K as obtained by the described method. In Fig. 2 the area of the sample where the nanostructuring took place can easily be identified. At the temperature of $T=8$ K, j_c is increased by 5.6×10^{10} A/m^2 or 22% in the structured part.

The result of the temperature dependence of the critical current density in the film grown on unpatterned STO as well as in the film grown on the structured part is shown in Fig. 3. It must be mentioned that each data point represents the average of a whole set of pixels of the image. Over the whole range of the measured temperature, j_c is increased on the structured part of the substrate. For temperatures below 37 K the offset between the two curves is nearly constant, whereas for higher temperatures, the slope of the structured part is larger leading to a decrease of the offset. In this representation it is difficult to obtain detailed information out of the graph. To get a deeper insight, a different form of presenting the data must be used.

According to the Ginzburg-Landau theory, the two characteristic lengths λ and ξ show a temperature dependence of the form $\lambda, \xi \propto (1-T/T_c)^{-1/2}$ for T close to T_c . This suggests an ansatz of the form

$$j_c \propto j_0(1-T/T_c)^s, \quad (1)$$

where j_0 and s are free parameters, to be generally checked with the measured data. To do so, the data is plotted in a

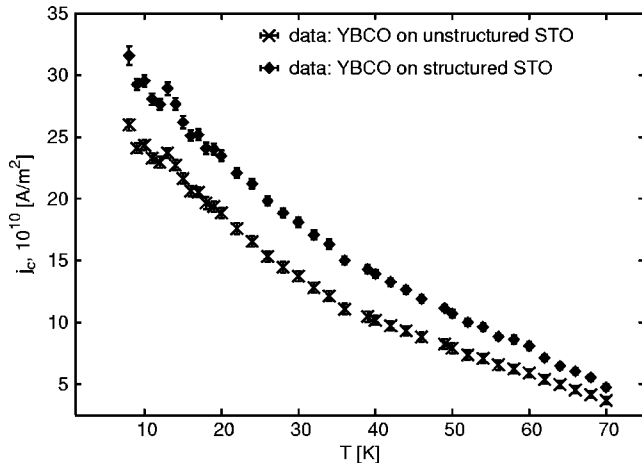


FIG. 3. Temperature dependence of the critical current density j_c for the part of the YBCO film grown on unstructured STO (\times) as well as for the part grown on the surface pattern (\blacklozenge). The error bars indicate the standard deviation of the evaluated data, where not visible the error is smaller than the representing symbol.

double-logarithmic manner with j_c over the reduced temperature $\tau = (1 - T/T_c)$.

Figures 4 and 5 show the results and also the corresponding fits of Eq. (1) to the data using the introduced double-logarithmic scale. The fitting was done using a least-mean-square algorithm. A two-step power-law behavior is found for both samples, YBCO on unstructured STO and YBCO on the structured substrate. The change in the exponent occurs very abruptly in a small temperature range around $T \approx 37$ K and the two-step nature of the temperature dependence is fulfilled within linewidth. Moreover, in this form of presentation one can easily identify differences in the power-law behavior of j_c in the YBCO film on the untreated substrate and on nanostructured STO in the low temperature regime. In case of the first one (Fig. 4), the critical current density decreases in the range from $T = 8 - 37$ K, following a quadratic power-law behavior with an exponent of s

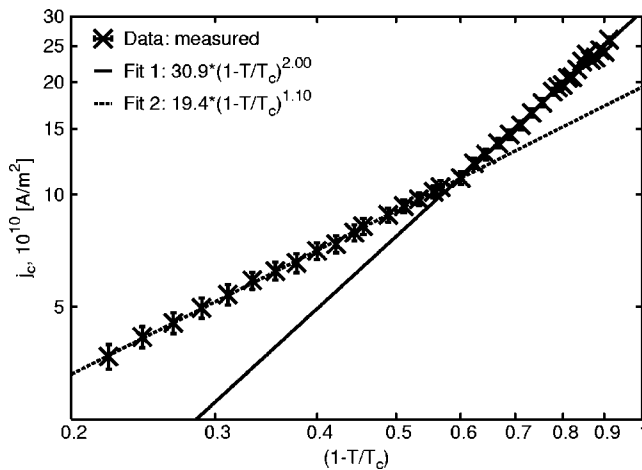


FIG. 4. Double-logarithmic plot of the critical current density in the film grown on the *unstructured* substrate over $\tau = (1 - T/T_c)$. The lines represent a power-law behavior $j \propto (1 - T/T_c)^s$ for $s = 2.0$ and $s = 1.1$, respectively, as obtained from fitting the data.

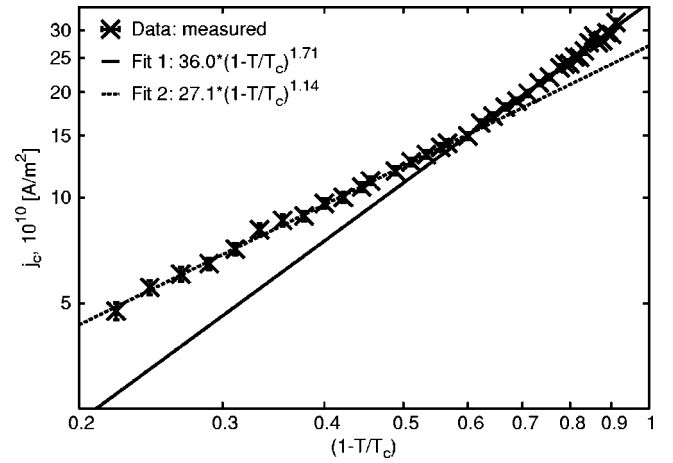


FIG. 5. Double-logarithmic plot of the critical current density in the film grown on the *structured* substrate. The lines represent a power-law behavior $j \propto (1 - T/T_c)^s$ for $s = 1.7$ and $s = 1.1$, respectively, as obtained from fitting the data.

$= 2.00 \pm 0.05$ and a factor j_0 of $j_0 = (30.9 \pm 0.3) \times 10^{10}$ A/m². While for temperatures above $T = 37$ K, the slope changes and j_c now shows a nearly linear decrease with temperature having an exponent of $s = 1.10 \pm 0.01$ and $j_0 = (19.4 \pm 0.1) \times 10^{10}$ A/m². The YBCO film on the structured part of the STO substrate (Fig. 5) behaves differently. For temperatures below $T = 37$ K, it exhibits an exponent of $s = 1.71 \pm 0.05$ with a j_0 of $j_0 = (36.0 \pm 0.4) \times 10^{10}$ A/m² while for higher temperatures the same linear power-law dependence like in the YBCO on untreated STO is found with $s = 1.14 \pm 0.01$. However, as expected from Fig. 3 j_0 is significantly larger than for the modified YBCO being $j_0 = (27.1 \pm 0.3) \times 10^{10}$ A/m².

A theoretical model for the temperature dependence of the critical current density in regular, epitaxially grown HTSC thin films has been suggested by Pashitskii *et al.*⁵ The model describes the temperature dependence of j_c in HTSCs assuming low-angle grain boundaries (LGB) between different growth islands of the film.

The existence of crystallites or grains and the corresponding intergranular LGB is emphasized by the fact that due to the Stranski–Krastanov mode for the growth of YBCO thin films on STO by pulsed laser deposition, a lot of intergranular links are created when the islands grow together.¹⁶ A second hint is provided by the temperature dependence of the critical current density across a single, well-defined LGB.^{3,17} There an exponent of $s = 3.0$ is found for j_c across a LGB with 3 degrees of misorientation angle and $s = 1.7$ for the unperturbed film.³ Note that these values have been obtained without the mentioned iteration method.

According to the model proposed by Pashitskii *et al.* (further referred to as LGB model), an epitaxial film is divided into crystalline blocks which exhibit a misorientation in the a - b plane. The LGBs in-between can be described by periodic chains of edge dislocations (ED) with a Burgers vector perpendicular to the LGB and a distance $d(\Theta)$ for the EDs determined, according to the Frank formula to $d(\Theta) = |B|/2 \sin(\Theta/2)$, by the misorientation angle Θ . For each ED of such a periodic chain, a local suppression of the superconducting order parameter ψ occurs in an area of several

coherence lengths $\xi_{ab}(t)$ width. This suppression reduces the critical current density across the LGB even if these areas, due to small angles Θ , do not overlap. On the other hand, the EDs can act as effective pinning sites for Abrikosov (or Abrikosov-like) vortices and, thus, lead to an increase of j_c . The temperature dependence of j_c in the framework of the LGB model has the form

$$j_c(\tau, \Theta) = \frac{j_0(\tau)}{2[\Gamma_1^2(\tau, \Theta) + 4]^{1/2}}. \quad (2)$$

Here Γ_1 is the transparency of the LGB which depends on the critical angle Θ_c and $\tau = (1 - T/T_c)$. When the distance between the EDs becomes so small that the areas of a suppressed ψ start to overlap, a conventional SNS type Josephson contact is formed along the LGB. The corresponding critical angle Θ_c is defined by

$$\Theta_c = (2\gamma/\pi)(|B|\sqrt{t}/\xi_{ab}) \quad (3)$$

with γ being a dimensionless coefficient and $\gamma = \pi/4$ under the condition $d(\Theta) = 2\xi(T)$ and assuming a cylindrical region with a radius of $\xi(T)$ for the suppressed ψ . According to the LGB model, two regimes for the temperature behavior of j_c , far from T_c , can be found. For large misorientation angles $\Theta > \Theta_c$, i.e., small distances $d(\Theta) < \xi(T)$ between the EDs, the areas of suppressed ψ overlap resulting in a temperature behavior of the form $j_c(\tau) \propto \tau^2$.^{5,18} On the other hand, if $\Theta < \Theta_c$, the parameter Γ_1 in Eq. (2) is independent of τ and Θ and $j_c(T)$ shows a behavior $j_c(\tau) \propto \tau^{3/2}$.⁵

To give an outlook, the temperature dependence of j_c will be compared to the introduced LGB model only in the lower temperature range, for higher temperatures the observed behavior must be described in a different way. For the unmodified part of the film, grown on the polished [100] STO surface, an exponent of $s = 2.00 \pm 0.05$ is found which is in perfect agreement with the predicted $j_c(T)$ behavior of a film with large misorientation angles ($\Theta > \Theta_c$).

The film grown on the nanostructured part of the substrate yields an exponent of $s = 1.71 \pm 0.05$. On the first glance, this does not fit into the theoretical framework since it's neither $s = 1.5$ (for $\Theta < \Theta_c$) nor $s = 2$ (for $\Theta > \Theta_c$). But due to the method of measurement the resulting value for $j_c(T)$ actually equals the integral of an area of at least $6 \times 6 \mu\text{m}^2$ (the resolution limit of the applied inversion scheme). So the value is probably given by an average of the two extreme situations. If both cases ($\Theta < \Theta_c$ and $\Theta > \Theta_c$) coexist in the film which is very likely since it is not completely homogenous one would expect to find an exponent between 1.5 and 2 depending on the distribution of the angles. This is exactly what is found. It seems that by nanostructuring, the LGBs are optimized with respect to their misorientation angles to be lower than the critical angle Θ_c and, thus, are about to exhibit higher critical currents. Nevertheless the found in-between value of $s = 1.71$ signifies that, for this system here, not all LGBs have been optimized to have $\Theta < \Theta_c$. Obviously there remains much potential to further improve the nanostructuring and by this improve more LGBs which would, according

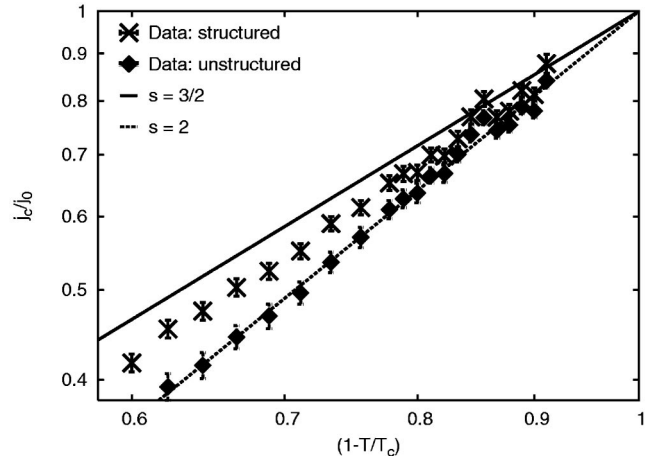


FIG. 6. Temperature dependence of the critical current compared with the theoretical predictions. The crosses show the measured $j_c(T)$ behavior on the structured part of the sample, the square indicates the result for the unstructured part. The given theoretical curves correspond to a misorientation angle $\Theta < \Theta_c$ resulting in an exponent of $s = 3/2$ indicated by the solid line and to the one with $\Theta > \Theta_c$ resulting in $s = 2$ represented by the dashed line, respectively, for the LGBs.

to the theoretical predictions, result in even higher critical current densities.

To present a better illustration of this good agreement with the theoretical model, Fig. 6 shows the measured data and the predicted behavior according to the LGB model for the temperature range $T = 8 - 37$ K in a normalized way.

The interpretation of the two-step behavior, whose existence cannot be neglected from the results presented here, is based on the assumption, that the change in the exponent is contributed to a change in the effective pinning mechanism. It must be mentioned that such a behavior has been observed before in epitaxially grown YBCO thin films.³ The scenario proposed here assumes that at low temperatures (below $T \approx 37$ K) the supercurrent is not limited due to depinning of the vortices but due to the properties, i.e., the angle Θ , of the LGBs between the crystallite blocks in the film. In accordance with the theoretical predictions the currents across the LGB are responsible for the limitation of j_c . However, for higher temperatures, no difference in the temperature dependence between the two parts of the sample was observed. For this regime, thermally activated depinning of the flux lines acts as a limiting factor for the critical current density. From theoretical models one obtains two possible scenarios. First correlated pinning (leading to $s = 1$) may be assumed or as a second possible scenario, δT_c pinning (giving $s = 1,166$) might occur.¹

In summary, detailed measurements of the temperature dependence of the critical current density in YBCO thin films grown on regular STO [100] surfaces and on nanostructured STO have been presented. It was possible to obtain the local critical current density in the film with very high precision. By comparing both results with each other and with theoretical models, the following general pinning mechanisms have been identified: for temperatures below $T \approx 37$ K, the vorti-

ces are tightly pinned at the EDs of the LGBs between the crystalline blocks. Since the LGBs exist for both investigated films, the critical current density depends on the transparency and the misorientation angle of the LGBs in this temperature range. These results imply that for the YBCO grown on the nanostructured substrate, the dislocation angles Θ of the LGBs are smaller than in the film grown on unpatterned STO. Above $T \approx 38$ K the dependence of j_c on the tempera-

ture changes, suggesting thermally activated depinning of the vortices.

The authors thank S. Leonhardt, E. H. Brandt, and G. Schütz for stimulating discussions, R. Spolenak for his help in nanostructuring the STO, S. Macke for implementing the iteration method, and G. Cristiani and H.-U. Habermeier for preparation of the excellent YBCO films.

*Electronic mail: s.brueck@gmx.org

- ¹G. Blatter, M. V. Feigel'man, V. B. Geshkenbein, A. I. Larkin, and V. M. Vinokur, *Rev. Mod. Phys.* **66**, 1125 (1994).
- ²C. Jooss, R. Warthmann, H. Kronmüller, T. Haage, H.-U. Habermeier, and J. Zegenhagen, *Phys. Rev. Lett.* **82**, 632 (1999).
- ³J. Albrecht, *Phys. Rev. B* **68**, 054508 (2003).
- ⁴Y. V. Fedotov, S. M. Ryabchenko, and A. P. Shakhov, *Low Temp. Phys.* **26**, 464 (2000).
- ⁵E. A. Pashitskii, V. I. Vakaryuk, S. M. Ryabchenko, and Y. V. Fedotov, *Low Temp. Phys.* **27**, 96 (2001).
- ⁶S. Leonhardt, J. Albrecht, R. Warthmann, H.-U. Habermeier, and H. Kronmüller, *Physica C* **341-348**, 1979 (2000).
- ⁷J. Albrecht, S. Leonhardt, H.-U. Habermeier, S. Brück, R. Spolenak, and H. Kronmüller, *Physica C* **404**, 18 (2004).
- ⁸J. Albrecht, S. Leonhardt, R. Spolenak, U. Täffner, H.-U. Habermeier, and G. Schütz, *Surf. Sci. Lett.* **547**, 847 (2003).
- ⁹S. Brück, J. Albrecht, H. Pfaff, G. Huber, R. Spolenak, G. Cristiani, H.-U. Habermeier, and G. Schütz (unpublished).
- ¹⁰H.-U. Habermeier, *Eur. J. Solid State Inorg. Chem.* **28**, 201 (1991).
- ¹¹C. Jooss, J. Albrecht, H. Kuhn, S. Leonhardt, and H. Kronmüller, *Rep. Prog. Phys.* **65**, 651 (2002).
- ¹²L. A. Dorosinskii, M. V. Indenbom, V. A. Nikitenko, Y. A. Ossip'yan, A. A. Polyanskii, and V. K. Vlasko-Vlasov, *Physica C* **203**, 149 (1992).
- ¹³C. Jooss, R. Warthmann, A. Forkl, and H. Kronmüller, *Physica C* **299**, 215 (1998).
- ¹⁴F. Laviano, D. Botta, A. Chiodoni, R. Gerbaldo, G. Ghigo, L. Gozzelino, S. Zannella, and E. Mezzetti, *Supercond. Sci. Technol.* **16**, 71 (2003).
- ¹⁵R. Warthmann, J. Albrecht, H. Kronmüller, and C. Jooss, *Phys. Rev. B* **62**, 15226 (2000).
- ¹⁶X.-Y. Zheng, D. H. Lowndes, S. Zhu, J. D. Budai, and R. J. Warmack, *Phys. Rev. B* **45**, 7584 (1992).
- ¹⁷H. Hilgenkamp and J. Mannhart, *Rev. Mod. Phys.* **74**, 485 (2002).
- ¹⁸A. Gurevich and E. A. Pashitskii, *Phys. Rev. B* **57**, 13878 (1998).